INTERNATIONAL JOURNAL OF RESEARCH
In Advanced Engineering Technologies

Volume 5, Issue 4 SEP 2016

A Fuzzy Based DC Current Flow Controller for Meshed Modular Multilevel Converter Multiterminal HVDC Grids

M.Padma[1], B.Kishan[2],T.Kranthi Kumar[3]
[1,2,3] Dept. of Electrical and Electronics Engineering
Avanthi Institute of Engineering & Technology
Hayathnagar, Ranga Reddy, Telangana, INDIA
Paddunany44@gmail.com[1], kishanbanoth2@gmail.com[2],kranthikumarthallapalli@gmail.com[3]

Abstract- In this paper, the design of a novel DC current flow controller (CFC) and evaluates the control performance of balancing and regulating the DC branch currents using the DC CFC in a meshed multi-terminal HVDC (MTDC) grid along with fuzzy logic controller was proposed. Here we are using fuzzy logic controller instead of using other controllers. The DC CFC consists of two identical full bridge DC-DC converters with the capacitors of the two converters being connected in parallel. The control performance of the DC CFC is tested on a meshed 3-terminal (3-T) HVDC grid, which is based on modular multilevel converters (MMC) using fuzzy logic controller. The DC branch current control in the meshed MTDC grid is achieved using the proposed control strategy of the DC CFC, and is verified through case studies on the real-time digital simulator (RTDS). Simulation was done by using MATLAB/Simulink software.

Index Terms— Capacitor voltage control, DC branch current control, DC current flow controller, HVDC transmission, meshed multi-terminal HVDC grid, modular multilevel converter, Fuzzy logic controller.

I. INTRODUCTION

The HVDC transmission technology is recognized as an advantageous approach for worldwide long-distance bulk-power transmissions with several HVDC[3]-[6] applications currently in use for MTDC technologies . China, at present, has two multi-terminal HVDC grids in operation. Due to its superiority in more efficiently utilizing and integrating renewable energy located in remote areas, MTDC technology has become more attractive in recent years compared to traditional point-to-point HVDCs[7]-[10]. The MTDC system can also be reconfigured into different topologies under faults, particularly after a faulted line is isolated, in order to increase the continuity and reliability of the power supply[10]. Regarding the MTDC technology. Basically, the VSC based technology has more advantages over the LCC based technology[11],[12]. This is because the vector controls of the VSC converters, which realizes the independent control of active and reactive power.

Hence, for the regulation of power, the VSC based MTDC system is considered more flexible, particularly in instances where the power flow reversal can be easily achieved by reversing the direction of DC currents rather than the reversal of DC voltages. Based on these characteristics, MTDC applications are being increasingly used in HVDC transmission. Radial interconnections of DC grids, in particular, are being predominantly considered [13] due to their simple configuration and control strategies for regulating power distribution. In a radial topology, there is only one path between two electric nodes, so the power is fully regulated.

Although the radial topology is simple and easy to realize, the meshed topology of DC grids, similar to that of AC grids, is considered as more favorable for real power applications[13]. This is because the meshed topology increases the redundancy of power transmission, which contributes to the enhancement of the reliability of the power system transmission. In a meshed DC grid, the total power exchanged at the converter DC side can be fully controlled; however, the DC current of each branch, depending on the voltage difference of two DC terminals and the resistance of the DC branch, may not be controllable. If there is no additional control strategy to balance the branch currents, the distribution of branch currents will be determined by Kirchhoff's laws.

There is a potential risk that one or more branches of a DC grid may become overloaded, while other branches may be underutilized, since more currents will inherently be delivered to the branch of lower resistance. Therefore, the complexity of the meshed DC grid leads to the potential problems, which are the main concerns of this paper. There are several control strategies for meshed MTDC grids that have been proposed in the literature. In different droop controllers have been investigated for MTDC grids including meshed topologies. It was found that while the active power of each terminal could be coordinated to a certain extent, the distribution of the DC current on each branch was incapable of being accurately controlled in the meshed grid. A power flow control device for

a meshed DC grid has been designed and demonstrated in[13].

In this work, the DC branch current is well controlled by switching on and off the variable resistance of the device. However, the power loss due to switch-in resistance is an undesirable outcome. Reference has presented a power flow control device that provides a detailed system configuration and basic control logic for a meshed DC. However, the control strategy in this device has not been comprehensively analyzed nor a detailed control strategy proposed. A conceptual DC control flow controller (CFC) has been proposed in which standard full-bridge DC-DC converters with low voltage ratings are used to design the controller. However, only a basic conceptualization of this control device is introduced, and the performance of the branch current control capability is not fully illustrated, while the operating principle and detailed control approach of the device are also not thoroughly investigated.

In this paper, the design of a DC CFC, particularly its detailed control strategy of branch currents, is proposed for a meshed 3-T MMC HVDC[10] grid. The DC CFC is established based on the concept. The objective of the DC CFC is to control the DC branch currents by transferring the additional power from the overloaded branch to the underutilized branch and to realize this objective with relatively low power losses. The DC branch currents can be regulated at a certain range using the proposed control. The validity of the proposed control strategy of the DC CFC is verified through case studies on the RTDS.

II. MESHED 3-T MMC-HVDC SYSTEM

A. System Configuration

A single-line schematic diagram of the investigated meshed 3-T MMC-HVDC system is shown in Fig. l(a). The three terminals are T1, T2, and T3. The MTDC system has three (3) identical MMCs. Each MMC, as shown in Fig. l(b), comprises six (6) converter arms and each arm has n series half-bridge SMs and one series inductor Larm per converter arm. Each SM includes an energy storage capacitor C and two switching valves (81,82). Only one switch is switched on during normal operation.

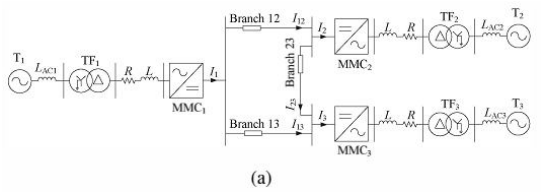

(a)

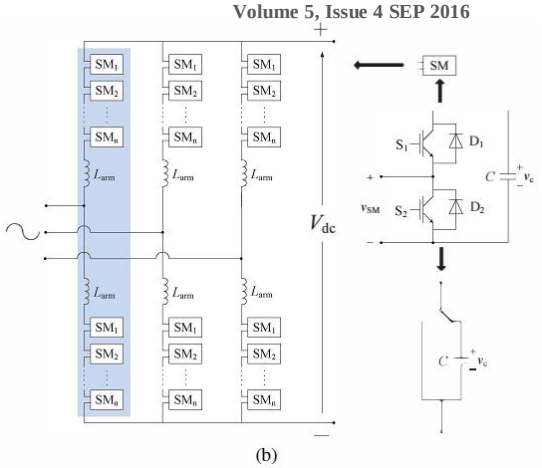

(b)

Fig. 1. Configuration of a meshed 3-T MMC-HVDC grid. (a) System configuration. (b) MMC configuration

Therefore, the output voltage VSM of each SM is either equal to the capacitor voltage Vc when the upper switch 81 is switched on, or equal to zero when the lower switch 82 is switched on. The MMC modeled in this paper has 6 SMs per converter arm. The MMC DC side is connected to the DC cable, while the MMC AC side is connected to an AC grid at each terminal through a series inductor and resistor as well as a three-phase transformer.

TABLE I: PARAMETERS OF THE 3-T MESHED MMC-HVDC SYSTEM IN FIG.1

Parameter	Value	Parameter	Value
Nominal AC source voltage	138 kV (L-N)	Nominal DC voltage	± 50 kV
L_{AC}	150 mH	MMCs rated capacity	150 MVA
Nominal AC frequency	50 Hz	L_{arm}	3 mH
Transformer voltage ratio	138 kV/30 kV (Y/Δ)	Number of SMs per arm	6
Transformer rating	150 MVA	Submodule capacitor	2,500 μF
Transformer leakage inductance	5%	Branch 12 cable resistance R_{12}	1 Ω
R	0.03 Ω	Branch 13 cable resistance R_{13}	2 Ω
L	1 mH	Branch 23 cable resistance R_{23}	1 Ω

For the DC system, it is a ±50 kV meshed 3-T DC grid. The DC cables are modeled as lumped resistors and the resistance of the DC cable between each terminal, as shown in Table I, is different. For the AC systems of the 3 terminals, their configurations and parameters are identical. Complete system parameters are shown in Table I.

B. Control Strategies of the MMCs

The MMCs are considered as VSC type converters. The converter level control of the model in this paper applies the classic vector control strategy. Both MMC1 and MMC2 apply constant active power control. For the sake of simplification of the system analysis, some assumptions are made: 1) the losses of the converters are neglected; 2) the AC system voltage is constant due to the connection

to the AC utility grid; 3) the MMC DC side current is regulated to be constant via the active power control. The total current imported from T 1 to the DC grid is kept at 1 kA, while the total current exported from the DC grid to T 2 is kept at 0.4 kA. MMC3 is controlled to maintain the DC voltage of T 3 at ±50 kY. The reactive power is controlled to be at 0 by all three MMCs.

If there is no additional strategy to control the DC branch current, the distribution of branch currents, for instance, h2, h3 and 123, of the DC grid, are uncontrollable. One or more branches, therefore, may become overloaded, while the other is insufficiently utilized. The principle of electric power transmission is to achieve a maximum utilization of the transmission line/cable within its transfer capability. Therefore, the control of the branch currents is inevitable and necessitates additional controllers.

Since the branch currents of a meshed DC grid are deter- mined by DC cable resistances and DC voltage differences between two terminals, two approaches can be used to control the branch current. One is to change the cable resistance by adding an additional resistor on the DC branch. However, this method significantly increases power losses, which are undesirable. The second method aims at changing the voltage difference between two DC terminals to regulate the branch current. This method is considered a preferable approach since the branch current control is achieved with acceptable low power losses.

C. Equivalent Power Flow Analysis of the Meshed MTDC Grid

The DC nominal voltage of T 3 is regulated at ±50 kV, via the control of MMC3. Hence, the DC voltage of T3, V3, is 100 kY. TI imports 1 kA to the DC grid, while T2 exports 0.4 kA from the DC grid. Thus, the DC currents h and 12 are 1 kA and 0.4 kA, respectively. The DC buses of MMCI and MMC2 can be simplified and regarded as two ideal DC current sources, while the DC bus of MMC3 can be considered as an ideal voltage source. The diagram in Fig. 2 presents the simplifications of the DC grid. An equivalent power flow analysis is conducted based on Fig. 2.

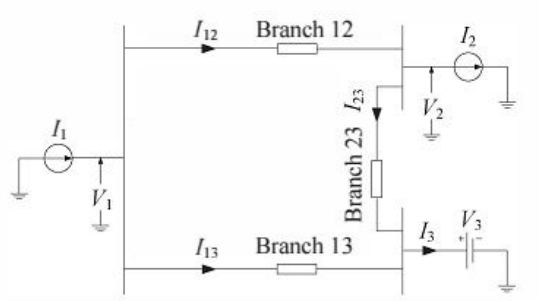

Fig. 2. Configuration of the 3-T MMC-HVDC grid.

Based on Kirchhoff Current Law (KCL), the currents in the meshed MTDC grid have the following relationships:

$$I_1 = I_{12} + I_{13} \quad (1)$$

$$I_3 = I_{13} + I_{23} \quad (2)$$

$$I_1 = I_2 + I_3 \quad (3)$$

According to Ohm's Law, the branch currents in Fig. 2 can be derived as:

$$I_{12} = \frac{V_1 - V_2}{R_{12}} \quad (4)$$

$$I_{13} = \frac{V_1 - V_3}{R_{13}} \quad (5)$$

$$I_{23} = \frac{V_2 - V_3}{R_{23}} \quad (6)$$

The values of h, 12, and V3 are determined by the control of MMCs, which means there are six unknown variables in (1)-(6). Therefore, all of their values can be obtained. The expressions of VI, V2 and h are derived in (7)-(9).

$$V_1 = V_3 + \frac{I_1 R_{13}[R_{12} + R_{23}] - I_2 R_{23} R_{13}}{R_1 + R_2 + R_3} \quad (7)$$

$$V_2 = V_3 + \frac{I_1 R_{23} R_{13} - I_2 R_{23}(R_{12} + R_{13})}{R_1 + R_2 + R_3} \quad (8)$$

$$I_3 = I_1 - I_2 \quad (9)$$

From the power flow analysis, it is observed that the branch current h2 is larger than 113. However, the cables in both branches are made from the same material and thus have the same transfer capability. Hence, Branch 12 is either overloaded or getting closer to its transfer limit, while Branch 13 is insufficiently utilized.

III. DC CURRENT FLOW CONTROLLER

A. Meshed MTDC System with a DC CFC

The DC CFC is equipped on Branch 12 and Branch 13. Fig. 3 shows a single-line schematic diagram of the developed meshed 3-T MMC-HVDC system with the DC CFC being equipped.

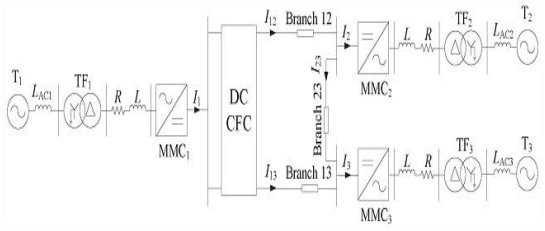

Fig. 3. 3-T MMC-HVDC system with the installation of the DC CFC.

The expected operating condition of the power transmission system is to keep each branch working at its optimal transfer capacity, and this is achievable by the control of the DC CFC.

B. Structure of the DC CFC

The detailed structure of the DC CFC installed between Branch 12 and Branch 13 is shown in Fig. 4.

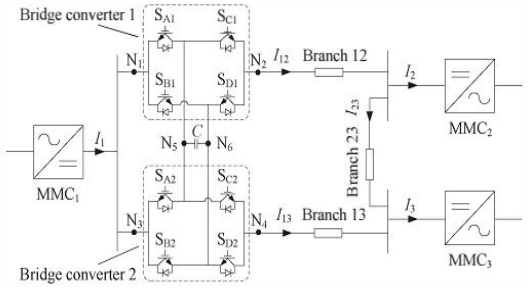

Fig. 4. Structure of the DC CFC

The DC CFC is composed of two identical full-bridge DC-DC converters. Fig. 5 shows the diagram of an independent full bridge DC-DC converter.

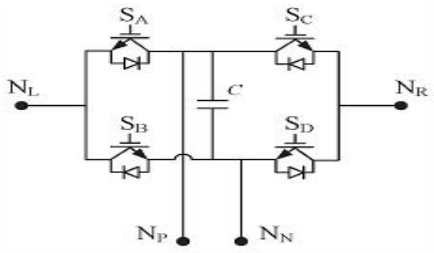

Fig. 5. Full bridge DC-DC converter.

A DC-DC converter has two legs and one energy storage capacitor in the middle. Each leg comprises two IGBTs with their anti-parallel diodes. SA and SB are on the same leg, while the other two (Sc and So) compose the other leg. Two switches on the same leg are switched complementary. Consequently, when SA is in its off state, SB is in the on state, which is the same for Sc and So. This operation manner ensures the two switches on the same leg are never off simultaneously. Under this switching specification, the current through the capacitor is always continuous. The capacitor has three operational states with different switching modes, bypassed, charged, and discharged, as shown in Table II. The capacitor is bypassed when both SA and Sc are on or both SB and So are on. The capacitor is charged when both SA and So are on, while the capacitor is discharged, when both SB and Sc are on.

TABLE II: SWITCHING MODES WITH CAPACITOR STATUS

Mode	Capacitor State	S_A	S_B	S_C	S_D
1	Bypassed	ON	OFF	ON	OFF
2	Bypassed	OFF	ON	OFF	ON
3	Charged	ON	OFF	OFF	ON
4	Discharged	OFF	ON	ON	OFF

The DC CFC is composed of the connection of two DC-DC converters. The interconnection points are the positive and negative side (Np, Nn) of the capacitor, respectively, as shown in Fig. 5.

IV. CONTROL STRATEGY OF THE DC CFC

The objective of using the DC CFC is to realize the control of the branch currents in the meshed 3-T MMC-HVDC grid. The equivalent power flow analysis of the meshed MTDC grid derived in Section II-C indicates that it is necessary to balance the current distribution of Branch 12 and Branch 13 through the control of the DC CFC. This is achieved by transferring additional power from Branch 12 to Branch 13 via the energy storage capacitor.

In addition, the voltage of a capacitor represents the energy stored in the capacitor. The energy of a capacitor can be approximately represented by its average voltage:

$$W_c = \frac{1}{2} C V_c^2 \qquad (10)$$

Vc is the average voltage stored in the capacitor. The power imported and exported of a capacitor is depicted in Fig. 6.

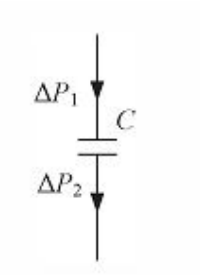

Fig. 6. Power imported and exported of a capacitor.

Under steady-state conditions, the power exchange of the interconnected capacitor is balanced, so

$$\Delta P_1 = \Delta P_2 \qquad (11)$$

That means the power imported to the capacitor equals to the power exported from the capacitor, so the power of the capacitor Pc is zero. As power is defined as the derivative of work, we have

$$\frac{dW_c}{dt} = P_c = 0 \qquad (12)$$

According to (10) and (12), the capacitor voltage should be controlled to maintain a certain value under steady-state conditions based on the operating condition of the DC CFC.

According to Table II, the capacitor of the DC-DC converter shown in Fig. 5 is charged with switching mode 3 and is discharged with mode 4. The duty ratio of each switch of the full-bridge DC-DC converter is DSJ (J = A, B, C, D) and the generated gating signal is Gs./. The gating signal is produced through the PWM by comparing the controlled signal with a saw-tooth wave. Two general operating states within two switching cycles are depicted in Fig. 7.

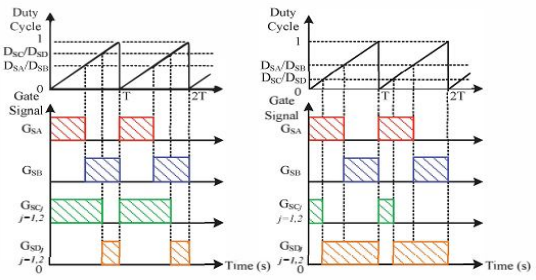

Fig. 7, Gate signal generation of each switch.

In Fig. 4, Branch 12 needs to transfer its power to Branch 13 by charging the interconnected capacitor, while Branch 13 needs to obtain the excess power from Branch 12 by discharging the interconnected capacitor. Due to the characteristics of complementary switching, only one switch on one leg needs to be controlled.

A. Branch Current Control

The branch current control is implemented through regulating the difference of the duty ratio between SA and SCI.

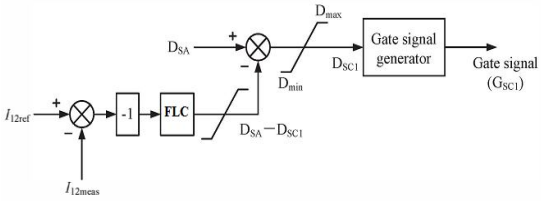

Fig. 8, Branch current control system.

As the switching performance is shown in Fig. 7, when the duty ratio difference DSA - DSCI is positive, the interconnected capacitor is charged and h2 becomes smaller. The measurement of branch current 12 (I12meas) is tracking its reference value (I12ref) by the application of a fuzzy controller. Fig. 8 illustrates the control approach.

B. Capacitor Voltage Control

The control of the capacitor voltage is similar to that of the branch current, via a fuzzy controller. The control approach is illustrated in Fig. 9. A positive (negative) tracking error signifies the measured capacitor voltage is smaller (larger) than its reference voltage and will result in a decrease (increase) in the generated duty ratio of SC2.

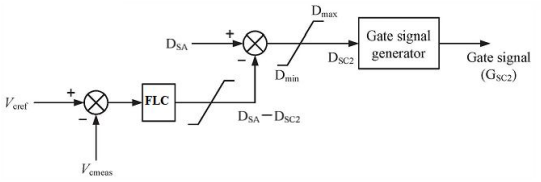

Fig. 9. Capacitor voltage control.

Thus, the interconnected capacitor will be charged (discharged) with switching mode 3 and Vc means will be increased (decreased) to track the control reference.

C. Start-up Process of the DC CFC

Initially, the DC CFC is in standby mode, i.e., the inter-connected capacitor is bypassed, so the capacitor voltage is zero and the branch currents are not controlled. 1meas (0.6 kA) is larger than the reference value (0.5 kA). When the DC CFC is started to control the branch currents, the duty ratios of SCI and SC2 generated are both decreased, leading to the charging of the interconnected capacitor. Hence, the voltage of the interconnected capacitor will be fast charged to the reference value

and 1meas will decrease during the charging process. A new steady-state condition will be achieved when the power exchanged between the capacitor is balanced, the voltage of the capacitor is well maintained and the branch current is regulated to the reference value.

D. Features of the DC CFC

The DC CFC with the proposed control has two main features:

I) Branch current balancing capability;

2) Branch current regulating capability.

V. FUZZY LOGIC CONTROLLER

In FLC, basic control action is determined by a set of linguistic rules. These rules are determined by the system. Since the numerical variables are converted into linguistic variables, mathematical modeling of the system is not required in FC.

The FLC comprises of three parts: fuzzification, interference engine and defuzzification. The FC is characterized as i. seven fuzzy sets for each input and output. ii. Triangular membership functions for simplicity. iii. Fuzzification using continuous universe of discourse. iv. Implication using Mamdani's, 'min' operator. v. Defuzzification using the height method.

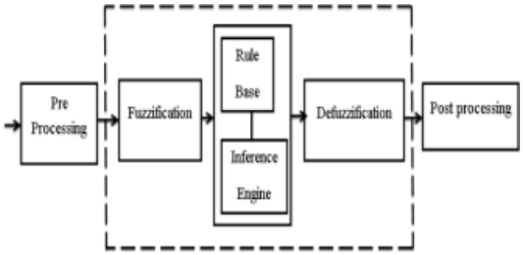

Fig.10.Fuzzy logic controller

Fuzzification: Membership function values are assigned to the linguistic variables, using seven fuzzy subsets: NB (Negative Big), NM (Negative Medium), NS (Negative Small), ZE (Zero), PS (Positive Small), PM (Positive Medium), and PB (Positive Big). The Partition of fuzzy subsets and the shape of membership *CE(k) E(k)* function adapt the shape up to appropriate system. The value of input error and change in error are normalized by an input scaling factor.

TABLE I: Fuzzy Rules

Change in error	Error						
	NB	NM	NS	Z	PS	PM	PB
NB	PB	PB	PB	PM	PM	PS	Z
NM	PB	PB	PM	PM	PS	Z	Z
NS	PB	PM	PS	PS	Z	NM	NB
Z	PB	PM	PS	Z	NS	NM	NB
PS	PM	PS	Z	NS	NM	NB	NB
PM	PS	Z	NS	NM	NM	NB	NB
PB	Z	NS	NM	NM	NB	NB	NB

In this system the input scaling factor has been designed such that input values are between -1 and +1. The triangular shape of the membership function of this arrangement presumes that for any particular *E(k)* input there is only one dominant fuzzy subset. The input error for the FLC is given as

$$E(k) = \frac{P_{ph(k)} - P_{ph(k-1)}}{V_{ph(k)} - V_{ph(k-1)}} \qquad (13)$$

$$CE(k) = E(k) - E(k\text{-}1) \qquad (14)$$

Inference Method: Several composition methods such as Max–Min and Max-Dot have been proposed in the literature. In this paper Min method is used. The output membership function of each rule is given by the minimum operator and maximum operator. Table 1 shows rule base of the FLC.

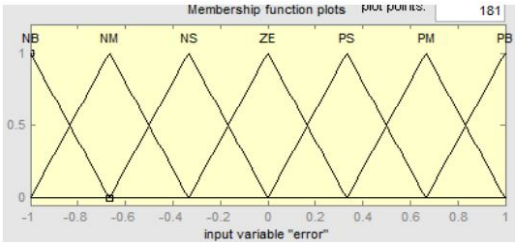

Fig.11.Membership functions

Defuzzification: As a plant usually requires a non-fuzzy value of control, a defuzzification stage is needed. To compute the output of the FLC, „height" method is used and the FLC output modifies the control output. Further, the output of FLC controls the switch in the inverter. In UPQC, the active power, reactive power, terminal voltage of the line and capacitor voltage are required to be maintained. In order to control these parameters, they are sensed and compared with the reference values. To achieve this, the membership functions of FC are: error, change in error and output

The set of FC rules are derived from

$$u=-[\alpha E + (1-\alpha)*C] \qquad (15)$$

Where α is self-adjustable factor which can regulate the whole operation. E is the error of the system, C is the change in error and u is the control variable. A

large value of error E indicates that given system is not in the balanced state. If the system is unbalanced, the controller should enlarge its control variables to balance the system as early as possible. One the other hand, small value of the error E indicates that the system is near to balanced state.

VI. SIMULATION RESULTS

The simulation system is the meshed 3-T MMC-HVDC system, as shown in Fig. 3, using the parameters provided in Table I. The structure of the DC CFC used in the simulation is the same as shown in Fig. 4. The interconnect capacitor C is 30 fLF, and the rated voltage of the IGBTs of the DC CFC is 10 kV.

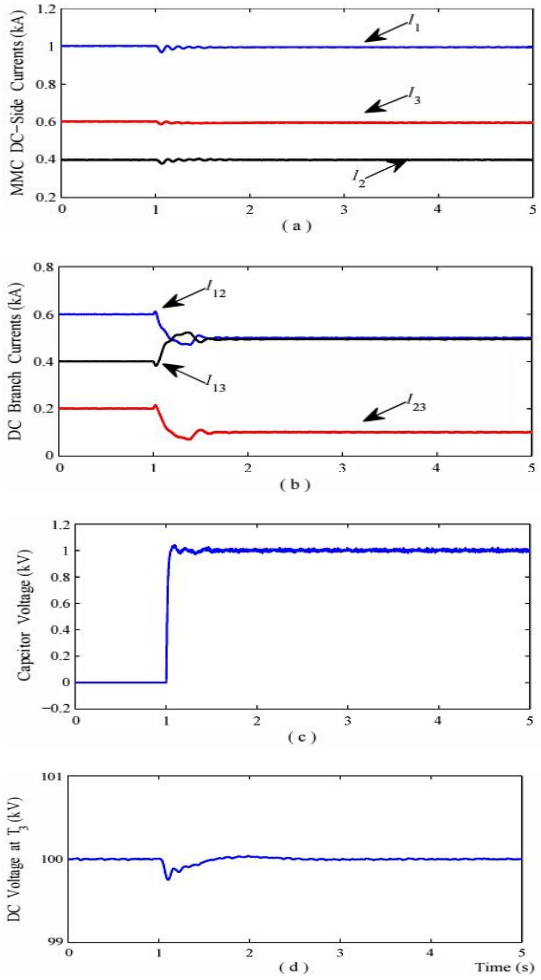

Fig. 11. System performance with branch current balancing control of the DC CFC. (a) h , h , I3 are the DC currents of Tl , T2 , and T3, respectively. (b) h2 , h3, and h3 are the DC currents of Branch 12, 13, and 23, respectively (c) Voltage of the interconnected capacitor (d) DC voltage at T3.

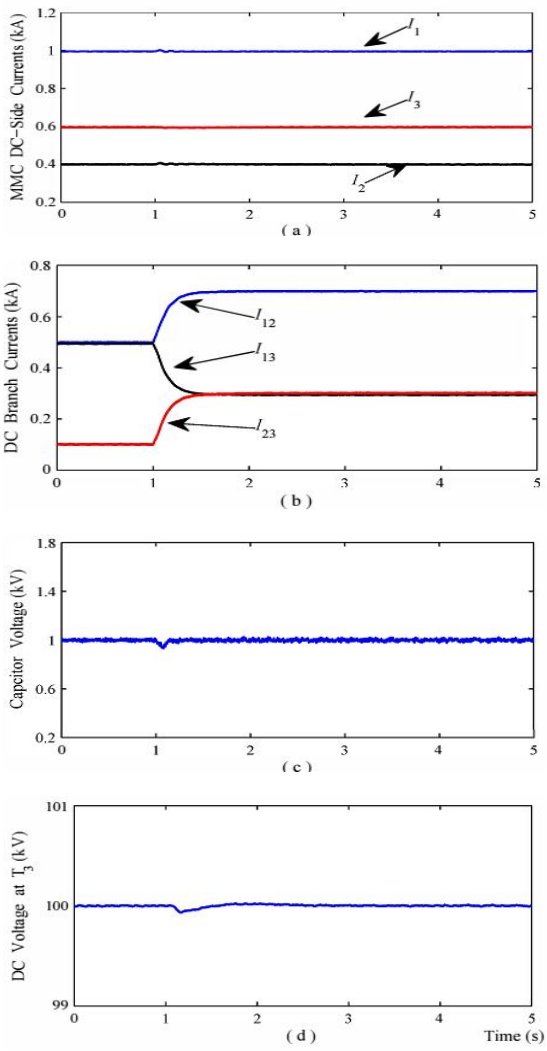

Fig. 12. System performance with branch current regulating control of the DC CFC. (a) h , Is are the DC currents of T 1, T 2 , and T 3, respectively. (b) h2 , h3, and /23 are the DC currents of Branch 12, 13, and 23, respectively (c) Voltage of the interconnected capacitor (d) DC voltage at T3.

VI. CONCLUSION

This paper has explained the design of a DC CFC, particularly its detailed control strategy, in order to control the branch currents in a meshed 3-T MMC-HVDC grid by using fuzzy logic controller. An equivalent power flow analysis of the 3-T meshed grid under the steady-state condition has been derived. It has been found that for the system without DC CFC, the branch currents are uncontrollable and one or more branches may become either overloaded or underutilized. The DC CFC has features of branch current balancing and regulating capability with the proposed control, which has been validated through case studies on the RTDS. This DC CFC with the proposed control can be regarded as an effective model for the branch

current control in a meshed DC grid. The simulation was done by using MATLAB/Simulink software.

REFERENCES

[1] M. P. Bahrman and B. K. Johnson, "The ABCs of HVDC transmission technologies," IEEE Power and Energy Magazine, vol. 5, no. 2, pp. 32-44, 2007.

[2] N. F1ourentzou, V. G. Agelidis, and G. D. Demetriades, "VSC-based HVDC power transmission systems: An overview," IEEE Transactions on Power Electronics, vol. 24, no. 3, pp. 592-602, 2009.

[3] T. M. Haileselassie and K. Uhlen, "Power system security in a meshed North Sea HVDC grid," Proceedings of the IEEE, vol. lOl, no. 4, pp. 978-990, 2013.

[4] D. Van Hertem and M. Ghandhari, "Multi-terminal VSC HVDC for the European supergrid: Obstacles," Renewable and Sustainable Energy Reviews, vol. 14, no. 9, pp. 3156-3163, 2010.

[5] G. Bathurst and P. Bordignan, "Delivery of the Nanao multiterminal VSC-HVDC system," presented at lET 11th International Conference on AC DC Power Transmission, Feb. 2015.

[6] X. J. Guo, S. S. Zhao, Y. H. Wang, G. Q. Bu, and Q. Guo, "Discussion on cascade-connected multi terminal UHVDC system and its application," in IEEE Power and Energy Society General Meeting, 2012, pp. 1-5.

[7] X. P. Zhang, "Multi terminal voltage-sourced converter-based HVDC models for power flow analysis," IEEE Transactions on Power Systems, vol. 19, no. 4, pp. 1877-1884, 2004.

[8] X. Chen, H. Sun, J. Wen, W. J. Lee, X. Yuan, N. Li, and L. Yao, "Integrating wind farm to the grid using hybrid multi terminal HVDC technology," IEEE Transactions on Industry Applications, vol. 47, no. 2, pp. 965-972, 2011.

[9] O. Gomis-Bellmunt, A. Egea-Alvarez, A. Junyent-Ferre, J. Liang, J. Ekanayake, and N. Jenkins, "Multiterminal HVDC-VSC for offshore wind power integration," in IEEE Power and Energy Society General Meeting, 2011, pp. 1-6.

[10] P. Wang, X. P. Zhang, P. F. Coventry, and Z. Li, "Control and protection strategy for MMC MTDC system under converter-side AC fault during converter blocking failure," Journal of Modern Power Systems and Clean Energy, vol. 2, no. 3, pp. 272-281, 2014.

[11] M. Davies, M. Dommaschk, J. Dorn, J. Lang, D. Retzmann, andD. Soerangr, "HYDC plus-basics and principle of operation," in SpecialEdition for Cigre Exposition, 2008.

[12] M. Saeedifard and R. Iravani, "Dynamic performance of a modular
multilevel back-to-back HVDC system," IEEE Transactions on Power
Delivery, vol. 25, no. 4, pp. 2903-2912, 2010
.

[13] Q. Mu, J. Liang, Y. Li, and X. Zhou, "Power flow control devices in
DC grids," in IEEE Power and Energy Society General Meeting, 2012,
pp. 1-7.

M.PADMA, completed post-graduation in Electrical power systems at Avanthi Institute of engineering & Technology, Hyderabad in 2016, and She completed graduation in EEE from KITSW, Nizamabad in 2013.

B.KISHAN, working as assistant professor in Avanthi Institute of Engineering & Technology, Hyderabad. He completed graduation in EEE department at MITS kodad, in 2009. He completed post graduated at Adam's engg. clg, paloncha, in 2013.

T. Kranthi Kumar, head of EEE Department in Avanthi Institute of engineering & technology, Hyderabad. He completed Graduation in EEE from Adam's Engineering College **(**Accredited by NBA), Paloncha. He completed M. Tech in P. Indra Reddy Memorial Engineering College in 2012. His papers published in International Journals, National and International Conferences Proceedings. And he is life member of Indian Society for Technical Education.Research area of interest is power quality, Renewable energy sources.